

Radiation damage free two-color X-ray ghost diffraction with atomic resolution

Zheng Li,^{1,2,3,*} Nikita Medvedev,^{1,2} Henry Chapman,^{1,2,4} and Yanhua Shih^{5,†}

¹Center for Free-Electron Laser Science, DESY, Notkestraße 85, D-22607 Hamburg, Germany

²Hamburg Centre for Ultrafast Imaging, Luruper Chaussee 149, D-22761 Hamburg, Germany

³SLAC National Accelerator Laboratory, Menlo Park, California 94025, USA

⁴Department of Physics, University of Hamburg, Jungiusstraße 9, D-20355 Hamburg, Germany

⁵Department of Physics, University of Maryland, Baltimore County, Baltimore, Maryland 21250, USA

The X-ray free electron lasers (XFEL) can enable diffractive structural determination of protein crystals or single molecules that are too small and radiation-sensitive for conventional X-ray analysis. However the electronic form factor could have been modified during the ultrashort X-ray pulse due to photoionization and electron cascade caused by the intense X-ray pulse. For general X-ray imaging techniques, to minimize radiation damage effect is of major concern to ensure faithful reconstruction of the structure. Here we show that a radiation damage free diffraction can be achieved with an atomic spatial resolution, by using X-ray parametric down-conversion (PDC), and two-color biphoton ghost imaging. We illustrate that formation of the diffractive patterns satisfies a condition analogous to the Bragg equation, with a resolution that could be as fine as the lattice length scale of several Å. Because the samples are illuminated by the optical photons of low energy, they can be free of radiation damage.

The advent of femtosecond X-ray free electron lasers has enabled diffractive structural determination of protein crystals or single molecules that are too small and radiation-sensitive for conventional X-ray analysis [1–3]. Using X-ray pulses of ~ 10 fs, sufficient diffraction signals could be collected before significant changes occur to the nanocrystals [1], however the electronic form factor could have been modified due to photoionization and electron cascade caused by the intense X-ray pulse [4], because $h\nu_X \gg h\nu_{\text{binding}}$, where $h\nu_X$ is the X-ray photon energy and $h\nu_{\text{binding}}$ is the electron binding energy, h is the Planck's constant. For general X-ray imaging techniques, to minimize radiation damage effect is of major concern of scientists, which guarantees a faithful reconstruction of the structure. Here we show that a radiation damage free diffraction is achievable with an atomic spatial resolution, by using X-ray parametric down-conversion (PDC)[5–7], and two-color biphoton ghost imaging [8–11]. A hard x-ray pulse are down-converted to a pair of x-ray and optical photon of wavelength λ_X and λ_o , the optical photons are sent to illuminate the sample crystals or molecules, and the scattered photons are collected with a bucket detector. Using the coincidence measurement of the ghost imaging procedure, the X-ray photons can form diffractive patterns on pixel detectors [9]. We illustrate that formation of the diffractive patterns satisfies a condition analogous to the Bragg equation, with a resolution that could be as fine as the lattice length scale of several Å. Because the samples are illuminated by the optical photons of low energy, they can be free of radiation damage. The ultra-bright property of XFEL should be crucial for realization of the proposed scheme, to ensure sufficient biphoton flux and signal strength. Since the diffraction pattern

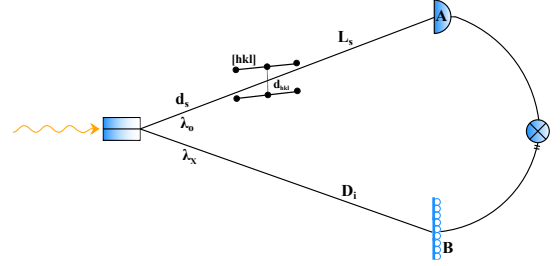


FIG. 1. Proposed layout for two-color biphoton ghost diffraction of X-ray and optical photon pair. The optical photons scatter off lattice planes with Miller index $[hkl]$ and inter-plane distance d_{hkl} .

formation is based on photon counting, the requirement for signal intensity is benign, we also show that the analogous Bragg condition can be satisfied with feasible experimental parameters.

An optical pulse and an X-ray pulse from X-ray PDC are oriented to illuminate a crystal in the optical arm and form diffractive patterns in the X-ray arm (Fig. 1). Without loss of generality, we assume that the signal photon has optical wavelength of $\lambda_s = \lambda_o$, and the idler photon has X-ray wavelength of $\lambda_i = \lambda_X$. As the optical photons scatter off lattice planes of inter-plane distance $d_{hkl} = d$, the condition for the X-ray photons to form peak in diffraction pattern is

$$d \left[\frac{1}{\sin \theta} - \frac{\sin \theta}{(\alpha + 1) \left(\frac{\lambda_i}{\lambda_s} \right)^2} \frac{|\rho_B|^2}{D_i^2} \right] = n\lambda_s, \quad (1)$$

where n is an integer, θ is the incident angle of the optical photon beam and lattice planes of a Miller index $[hkl]$ (Fig. 2). θ has a fixed relation with the orientation angle of the X-ray beam determined from the phase

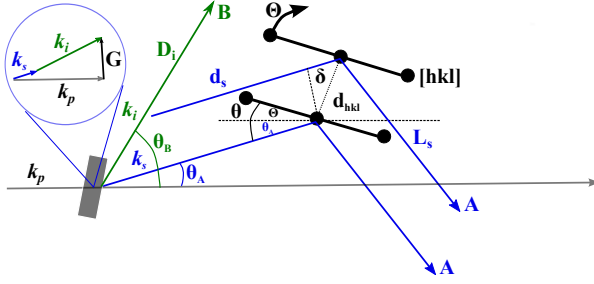


FIG. 2. Schematic of the proposed experiment. The sample is rotated by Θ , and its lattice plane forms an angle of θ with the incident optical beam in arm A. The relative angle of the X-ray beam (arm B) with the pump beam is determined from the phase matching diagram, $\mathbf{k}_s + \mathbf{k}_i = \mathbf{k}_p + \mathbf{G}$, where \mathbf{G} is a reciprocal lattice vector orthogonal to certain atomic planes of a nonlinear crystal, \mathbf{k}_s , \mathbf{k}_i and \mathbf{k}_p are the wave vectors of the signal, idler and pump fields.

matching condition. α is defined as $\frac{d_s}{D_i} = \alpha \frac{\lambda_i}{\lambda_s}$.

The biphoton coincidence counting rate of the bucket detector A and the pixel detector can be written as [7, 9, 11],

$$R_c = \frac{1}{T} \int dt_A dt_B S(t_B, t_A) \int_{\sigma_A} d^2 \rho_A \sigma_B \times \text{tr} \left[E_A^{(-)} E_B^{(-)} E_B^{(+)} E_A^{(+)} \rho \right], \quad (2)$$

where $S(t_B, t_A)$ is the coincidence time function that vanishes unless $0 \leq t_B - t_A \leq T$, ρ_A is on the plane of bucket detector A with area σ_A , σ_B is the area of the pixel detector B. ρ is the density matrix of the biphoton state on the output plane of the nonlinear crystal. $E_j^{(+)} = E^{(+)}(\mathbf{r}_j, t_j)$, $j = A, B$ is the positive frequency part of the photon field, and $E_j^{(-)} = (E_j^{(+)})^\dagger$. Provided that the Bragg equation (Eq. 1) and phase matching condition are satisfied, by coincidence photon counting in a joint measurement of bucket detector A and pixel detector B, diffraction patterns can be formed with coincidence count rate. For the schematic configuration in Fig. 1, the coincident count rate at ρ_B in the plane of pixel detector is [12]

$$R_c(\rho_B) = \frac{1}{T} \int dt_A dt_B S(t_B, t_A) \frac{\gamma^2 \psi_0^2 \sigma_A \sigma_B}{2\pi^2 \lambda_s^4 R_s^4 L_s^4} \times \left| \int d\mathbf{v}_s e^{i\mathbf{v}_s \cdot \mathbf{r}_{BA}} \text{sinc}(\mathbf{v}_s \cdot \mathbf{D}_{si} \frac{L}{2}) \right|^2 \times \left\{ 1 - \frac{\lambda_s L_s^2}{4d \sin \theta \sigma_A} \sin \left[\frac{2\pi}{\lambda_s R_s} d \left(x - \frac{R_s + L_s}{2L_s} d \right) \right] \right\} \quad (3)$$

$R_c(\rho_B)$ defines the diffraction pattern formed at the pixel detector. γ and D_{si} are parameters of the X-ray PDC process [12], $D_{si} = \frac{1}{U_s} - \frac{1}{U_i}$, U_s and U_i are the group ve-

locity of the signal and idler photon inside the nonlinear crystal of length L . $\tau_{BA} = \tau_B - \tau_A$, where $\tau_i = t_i - \frac{r_i}{c}$, $i = A, B$. ψ_0 is the scattering amplitude of an atom in the lattice with the optical photons, and the effective optical path length from the sample to the pixel detector B, $R_s = \frac{\lambda_i}{\lambda_s} D_i + d_s$. We assume the phase matching condition to be $\Omega_s n_s(\Omega_s) + \Omega_i n_i(\Omega_i) = c k_p$, ignoring \mathbf{G} for simplicity, \mathbf{G} can be restored for a given experimental configuration. The frequency of the signal field is $\omega_s = \Omega_s + \nu_s$, with ν_s characterizing the deviation from the central frequency Ω_s of phase matching condition, and $\nu_s = -\nu_i$. Although the period of the diffraction pattern $(\frac{\lambda_s}{d}) R_s$ could be too large for observation of higher order diffraction peaks, the 0th and 1st order patterns are sufficient to determine the inter-plane distance d , and to resolve the crystal structure.

To validate the experimental feasibility, we assume an X-ray pulse of 8 keV ($\lambda_i = 1.5\text{\AA}$) and an optical pulse of 1.55 eV ($\lambda_s = 8000\text{\AA}$) [5]. We consider the 0th order diffraction, with $|\rho_B| = \frac{R_s + L_s}{2L_s} d \ll D_i$, we take $\rho_B \simeq 0$. The Bragg condition is satisfied by rotating the crystal by Θ to form an angle $\theta = \theta_A + \Theta$ with the incident beam of optical photons (Fig. 2). Eq. 1 can be approximated as $\frac{d}{\sin \theta} = n \lambda_s$, where n is an integer. Taken $d = 8\text{\AA}$, we have $\theta_{n=1} - \theta_{n=2} = 500\mu\text{rad}$, which is within the resolution capability of $10\mu\text{rad}$ for state-of-art diffractometer [5]. For an experimental scenario of nanocrystal injection by liquid jet [1], which effectively forms a "virtual powder diffraction" patterns, a pixel pnCCD detector placed with a distance of $10m$ should give $5000\mu\text{m}$ separation between Bragg peaks. The resolution requirement can be satisfied with the pixel pnCCD detector of $75\mu\text{m}$ pixel pitch [1]. The requirement to the spectral and angular resolution of the diffractometer determined by $\frac{\Delta d}{d} + \cot \theta \Delta \theta = \frac{\Delta \lambda_s}{\lambda_s}$, which is on the same scale of the conventional Bragg equation. For nanocrystals with size L , the Scherrer equation is found to be [12]

$$B = 2\Delta\theta = \frac{2\lambda_s \sin^2 \theta}{L \cos \theta}, \quad (4)$$

which determines the width B of Bragg peaks. We present a simulated ghost diffraction pattern in Fig. 3, which shows resolvable Bragg peaks. The optical photon energy of 4 eV may fall below band gap of the crystal, and significant absorption can be avoided. For Bragg peaks appearing at small angles as in Fig. 3, the reduction of peak intensity due to the thermal Debye-Waller factor could be negligible. Thus the proposed two-color biphoton ghost diffraction scheme could eventually achieve atomic scale resolution without radiation damage.

The physical mechanism of the two-color biphoton ghost diffraction may be understood from the particle nature of the optical and X-ray photons. The op-

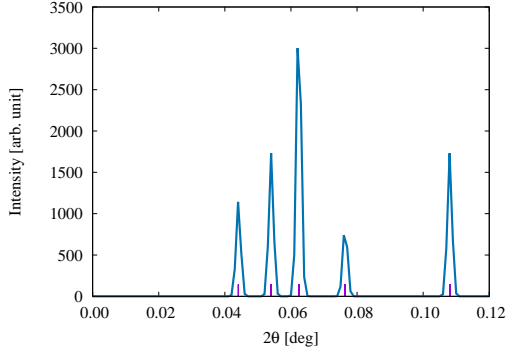


FIG. 3. Simulated two-color biphoton ghost diffraction from a body centered cubic crystal with lattice constant $a = b = c = 8\text{\AA}$. Optical photons of 4 eV are used to illuminate the sample crystal. The broadening of Bragg peaks is determined by Scherrer equation from a nanocrystal of 100 nm size.

tical photons scatter with the atoms in a nanocrystal or molecule, the momentum transfer of the scattering alters the momentum of their partner X-ray photons, which then form Bragg peaks. Thus the Bragg peak formation in the proposed scenario depends on the quantum product state of the optical and X-ray photons. As we could see in Fig. 3, although the Bragg peak separations could be within the resolution of state-of-art diffractometer, they are two orders of magnitude smaller than that of conventional X-ray Laue diffraction. Because the momentum of X-ray photon altered by the scattering of optical photon with the atoms is on a smaller scale than that of Laue diffraction, we have

$$\frac{|\mathbf{q}_{\text{biphoton}}|}{|\mathbf{k}_X|} < \frac{|\mathbf{q}_{\text{Laue}}|}{|\mathbf{k}_X|}. \quad (5)$$

Bragg peaks can not form in Laue diffraction with optical photon illumination, because the Bragg condition of Laue diffraction, $n\lambda/2d = \sin\theta \leq 1$, requires photon wavelength λ comparable to the distance between lattice planes. A possible route to enhance resolution of the two-color biphoton ghost diffraction is to magnify the momentum transfer in the X-ray photon arm by a certain optical method, in order to achieve larger Bragg peak separation.

Because the X-ray PDC and the sum-frequency generation (SFG) processes [5] are subject to the same nonlinear susceptibility, we can expect the feasibility of biphoton production with similar $\frac{\lambda_s}{\lambda_i}$ ratio. However, because the frequency of the optical photon is much lower than the X-ray photon, $\omega_o \ll \omega_X$, the experiment would suffer from suppression of photon-bound

electron scattering cross sections from the Thomson cross section σ_T of X-ray photons, which see the crystal as a periodic collection of free electrons since $\omega_X \gg \omega_{\text{binding}}$. The photon-bound electron cross section of a photon of frequency ω , $\sigma(\omega) = \sigma_T \frac{\omega^4}{(\omega_0^2 - \omega^2)^2 + \omega^2 \gamma^2}$ implies that the frequency of optical photons should be close to the resonance frequency ω_0 of atomic state, while being slightly detuned from the spectrum of resonance frequencies to avoid strong photoabsorption effect. In this sense, the optical photons in the ultraviolet (UV) and extreme ultraviolet (XUV) regime may not be the most favorable for the two-color biphoton ghost diffraction. In order to achieve sufficient photon counting rate, the multilayer structure instead of nonlinear crystal should be applied to enhance the quantum efficiency of X-ray PDC, and thus reach sufficient biphoton flux.

In conclusion, we have theoretically described a mechanism to realize x-ray diffraction with a super-resolution at atomic scale by two-color biphoton ghost imaging. Because the material object is irradiated by photons of optical wavelength, the proposed scheme can be free of radiation damage of x-ray photons.

We thank the Hamburg Centre for Ultrafast Imaging for financial support. We thank Nina Rohringer, Ivan Vartanyants, Ralf Röhlsberger, Robin Santra and Ludger Inhester for commenting on various aspects of the study. Z.L. is thankful to the Volkswagen Foundation for a Paul-Ewald postdoctoral fellowship, Oriol Vendrell and Todd Martínez for assistance.

* zheng.li@cfel.de

† shih@umbc.edu

- [1] A. Barty et al., *Nature Photonics* **6**, 35 (2012).
- [2] J. Spence, *Nature Photonics* **2**, 390 (2008).
- [3] Y. Nishino, Y. Takahashi, N. Imamoto, T. Ishikawa, and K. Maeshima, *Phys. Rev. Lett.* **102**, 018101 (2009).
- [4] H. Quiney and K. A. Nugent, *Nature Phys.* **7**, 142 (2011).
- [5] T. E. Glover et al., *Nature* **488**, 603 (2012).
- [6] K. Tamasaku, K. Sawada, E. Nishibori, and T. Ishikawa, *Nature Phys.* **7**, 705 (2011).
- [7] S. Shwartz et al., *Phys. Rev. Lett.* **109**, 013602 (2012).
- [8] T. B. Pittman, Y. H. Shih, D. V. Strekalov, and A. V. Sergienko, *Phys. Rev. A* **52**, R3429 (1995).
- [9] A. Strekalov, A. V. Sergienko, D. N. Klyshko, and Y. H. Shih, *Phys. Rev. Lett.* **74**, 3600 (1995).
- [10] G. Scarcelli, V. Berardi, and Y. H. Shih, *Phys. Rev. Lett.* **96**, 063602 (2006).
- [11] M. H. Rubin and Y. H. Shih, *Phys. Rev. A* **78**, 033836 (2008).
- [12] Supplemental material .

SUPPLEMENTAL MATERIAL
Radiation damage free two-color X-ray ghost diffraction with atomic resolution

Zheng Li,^{1,2,3,*} Nikita Medvedev,^{1,2} Henry Chapman,^{1,2,4} and Yanhua Shih^{5,†}

¹*Center for Free-Electron Laser Science, DESY, Notkestraße 85, D-22607 Hamburg, Germany*

²*Hamburg Centre for Ultrafast Imaging, Luruper Chaussee 149, D-22761 Hamburg, Germany*

³*SLAC National Accelerator Laboratory, Menlo Park, California 94025, USA*

⁴*Department of Physics, University of Hamburg, Jungiusstraße 9, D-20355 Hamburg, Germany*

⁵*Department of Physics, University of Maryland,
Baltimore County, Baltimore, Maryland 21250, USA*

* zheng.li@cfel.de

† shih@umbc.edu

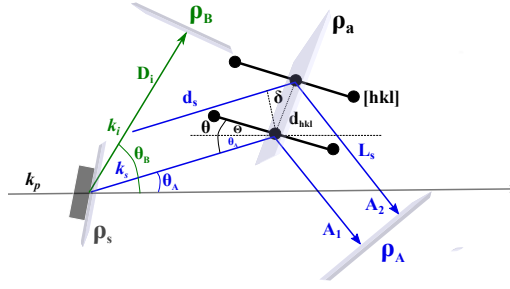


FIG. 1. Proposed layout for two-color biphoton ghost diffraction of X-ray and optical photon pair. ρ_A , ρ_B , ρ_s , ρ_a are vectors on the planes of the bucket detector A, the pixel detector B, the X-ray PDC source and atoms in the sample.

The supplemental material is divided into two sections. Section I describes explicitly the analogous Bragg equation, Eq. (1) and the joint photon counting rate for diffraction pattern formation, Eq. (2). Section II illustrate a simple kinematic description of Laue diffraction for the completeness of the theory presented in Section I. Section III treats the broadening effect of Bragg peaks.

I. BRAGG EQUATION FOR TWO-COLOR BIPHOTON DIFFRACTION

We assume paraxial approximation for the wave vectors of modes $|\mathbf{k}\rangle$ of the photon field, $\mathbf{k} = \sqrt{k^2 - \kappa^2} \hat{z} + \kappa$, with $k = \frac{\omega}{c} \gg \kappa$. The biphoton coincidence counting rate of the bucket detector A and the pixel detector can be written as [1–3],

$$R_c(\rho_B) = \frac{1}{T} \int dt_A dt_B S(t_B, t_A) \int_{\sigma_A} d^2 \rho_A \sigma_B \text{tr} \left[E_A^{(-)} E_B^{(-)} E_B^{(+)} E_A^{(+)} \rho \right], \quad (1)$$

where $S(t_B, t_A)$ is the coincidence time function that vanishes unless $0 \leq t_B - t_A \leq T$, ρ_A is on the plane of bucket detector A with area σ_A , σ_B is the area of the pixel detector B. ρ is the density matrix of the biphoton state on the output plane of the nonlinear crystal. $E_j^{(+)} = E^{(+)}(\mathbf{r}_j, t_j)$, $j = A, B$ is the positive frequency part of the photon field, and $E_j^{(-)} = (E_j^{(+)})^\dagger$.

We compute the photon fields at the plane of the bucket detector A and the pixel detector B, $E_A^{(+)}$ and $E_B^{(+)}$,

$$\begin{aligned} E_A^{(+)} &= \sum_{\mathbf{k}_s} g(\kappa_s, \omega_s, \rho_A, z_s) \hat{a}_s(\mathbf{k}_s) e^{-i\omega_s t_A} \\ E_B^{(+)} &= \sum_{\mathbf{k}_i} g(\kappa_i, \omega_i, \rho_B, z_i) \hat{a}_i(\mathbf{k}_i) e^{-i\omega_i t_B}, \end{aligned} \quad (2)$$

where $z_s = d_s + L_s$ and $z_i = D_i$ are the full optical path lengths for the signal and idler photon. $\hat{a}_p^\dagger(\mathbf{k})$ and $\hat{a}_p(\mathbf{k})$ are operators of signal and idler photon field in a specific mode at the output plane of the nonlinear crystal, with commutators,

$$[\hat{a}_p(\mathbf{k}), \hat{a}_q^\dagger(\mathbf{k}')] = \delta_{p,q} \delta_{\omega, \omega'} \delta_{\kappa, \kappa'}. \quad (3)$$

$g(\kappa, \omega, \rho, z)$ is the Green's function for a specific mode of photon field.

Assume two atoms in two lattice planes of Miller index $[hkl]$ with distance $d = d_{hkl}$ are in a plane a , ρ_a is a vector in this plane (Fig. S1), and the photon-atom scattering amplitude is $t(\rho_a)$, we shows that $E_A^{(+)}$ and $E_B^{(+)}$ can be written as [4],

$$\begin{aligned} E_A^{(+)} &= \sum_{\mathbf{k}} \int d^2 \rho_{s'} \int d^2 \rho_a \frac{-ik}{2\pi d_s} e^{ikd_s} e^{i\kappa \cdot \rho_{s'}} e^{i\frac{\kappa}{2d_s} |\rho_a - \rho_{s'}|^2} t(\rho_a) \frac{-ik}{2\pi L_s} e^{ikL_s} e^{i\frac{\kappa}{2L_s} |\rho_A - \rho_a|^2} e^{-i\omega t_A} \hat{a}_s(\mathbf{k}) \\ E_B^{(+)} &= \sum_{\mathbf{k}} \int d^2 \rho_s \frac{-ik}{2\pi D_i} e^{ikD_i} e^{i\kappa \cdot \rho_s} e^{i\frac{\kappa}{2D_i} |\rho_s - \rho_B|^2} e^{-i\omega t_B} \hat{a}_i(\mathbf{k}). \end{aligned} \quad (4)$$

Denote $G(|\alpha|, \beta) = e^{i\frac{\beta}{2}|\alpha|^2}$, its two-dimensional Fourier transformation is

$$\int d^2\alpha G(|\alpha|, \beta) e^{i\gamma \cdot \alpha} = i\frac{2\pi}{\beta} G(|\gamma|, -\frac{1}{\beta}). \quad (5)$$

The photon field $E_A^{(+)}$ and $E_B^{(+)}$ can be then written as

$$\begin{aligned} E_A^{(+)} &= \sum_{\mathbf{k}} \int d^2\rho_a \frac{1}{i\lambda L_s} t(\rho_a) G(|\rho_a - \rho_A|, \frac{k}{L_s}) e^{i\kappa \cdot \rho_a} G(|\kappa|, -\frac{d_s}{k}) e^{i(kz_s - \omega t_A)} \hat{a}_s(\mathbf{k}) \\ E_B^{(+)} &= \sum_{\mathbf{k}} G(|\kappa|, -\frac{D_i}{k}) e^{i\kappa \cdot \rho_B} e^{i(kz_i - \omega t_B)} \hat{a}_i(\mathbf{k}). \end{aligned} \quad (6)$$

With Eq. 6, we can obtain explicitly the second-order coherence function in Eq. 1,

$$\begin{aligned} G_{AB} &= \text{tr} [E_A^{(-)} E_B^{(-)} E_B^{(+)} E_A^{(+)} \rho] \\ &= |\langle 0 | E_B^{(+)} E_A^{(+)} | \Psi \rangle|^2 \\ &\equiv |U_{AB}|^2, \end{aligned} \quad (7)$$

where $|\Psi\rangle$ is the biphoton state vector. Without loss of generality, we ignore here the reciprocal lattice vector \mathbf{G} of the nonlinear crystal, which can be added for a given experimental configuration. Suppose the phase matching condition is satisfied for $\omega_p n_p(\omega_p) - \Omega_s n_s(\Omega_s) - \Omega_i n_i(\Omega_i) = 0$, with $K_j = \frac{\Omega_j}{c}$, and deviation from the central frequency $\omega_j = \Omega_j + \nu_j$, $j = s, i$. Frequency and spatial filtering guarantees $\nu_j \ll \Omega_j$ and $\kappa_j \ll K_j$, thus we have

$$\mathbf{k}_j = \kappa_j + (K_j + \frac{\nu_j}{c} + \frac{\nu_j^2}{2\Omega_j c} - \frac{\kappa_j^2}{2K_j}) \hat{e}_z \simeq \kappa_j + (K_j + \frac{\nu_j}{c}) \hat{e}_z. \quad (8)$$

Taken Eqs. 6 and 7, we have

$$\begin{aligned} U_{AB} &= \frac{1}{i\lambda_s L_s} e^{i(K_s z_s + K_i z_s - \Omega_s t_A - \Omega_i t_B)} \left[\sum_{\mathbf{k}_s, \mathbf{k}_i} g'_A(\rho_A, \nu_s, \kappa_s) g'_B(\rho_B, \nu_i, \kappa_i) \langle 0 | \hat{a}_s(\mathbf{k}_s) \hat{a}_i(\mathbf{k}_i) | \Psi \rangle \right] \\ &\equiv \frac{1}{i\lambda_s L_s} e^{i(K_s z_s + K_i z_s - \Omega_s t_A - \Omega_i t_B)} U'. \end{aligned} \quad (9)$$

Using a first-order perturbation theory, the biphoton amplitude from a PDC process is shown to be [2, 5],

$$\langle 0 | \hat{a}_s(\mathbf{k}_s) \hat{a}_i(\mathbf{k}_i) | \Psi \rangle = -i(2\pi)^3 \gamma \delta(\nu_s + \nu_i) \delta(\kappa_s + \kappa_i) \text{sinc}(\nu_s D_{si} \frac{L}{2}), \quad (10)$$

where $\gamma = \frac{\chi^{(2)} E_p L}{2U_s U_i} \sqrt{\frac{\Omega_s \Omega_i T_s T_i c^2}{n_s n_i}}$, $\chi^{(2)}$ is the second-order susceptibility of the nonlinear crystal, U_j is the group velocity of the signal and idler photon inside the nonlinear crystal of length L , T_j are their transmission coefficients. Using the relation [2]

$$\begin{aligned} \sum_{\mathbf{k}_s} &\rightarrow \frac{V}{(2\pi)^3} \int d\mathbf{k}_s = \frac{V}{(2\pi)^3} \int d^2\kappa_s \int d\omega_s \frac{dk_{s,z}}{d\omega_s} = \frac{V}{(2\pi)^3 c} \int d^2\kappa_s \int d\nu_s \\ \hat{a}_s(\mathbf{k}_s) &\rightarrow \frac{c}{V} \hat{a}_s(\kappa_s, \nu_s), \end{aligned} \quad (11)$$

we can write U' in Eq. 9 as

$$\begin{aligned} U' &= -i(2\pi)^{-3} \gamma \int d\nu_s e^{i\nu_s \tau_{BA}} \text{sinc}(\nu_s D_{si} \frac{L}{2}) \int d^2\rho_a \int d^2\kappa_s G(|\kappa_s|, -\frac{D_i}{k_i}) e^{-i\kappa_s \cdot \rho_B} G(|\kappa_s|, -\frac{d_s}{k_s}) e^{i\kappa_s \cdot \rho_a} \\ &\quad \times t(\rho_a) G(|\rho_a|, \frac{k_s}{L_s}) G(|\rho_A|, \frac{k_s}{L_s}) e^{-i\frac{k_s}{L_s} \rho_a \cdot \rho_A} \\ &\equiv -i\gamma \int d\nu_s e^{i\nu_s \tau_{BA}} \text{sinc}(\nu_s D_{si} \frac{L}{2}) \int d^2\rho_a I_{\kappa} t(\rho_a) G(|\rho_a|, \frac{k_s}{L_s}) G(|\rho_A|, \frac{k_s}{L_s}) e^{-i\frac{k_s}{L_s} \rho_a \cdot \rho_A} \end{aligned} \quad (12)$$

Define the effective sample-to-pixel detector path length $R_s = d_s + \frac{\lambda_i}{\lambda_s} D_i$, I_K in Eq. 12 can be rewritten as

$$\begin{aligned} I_K &= \frac{1}{(2\pi)^3} \int d^2 \kappa_s G(|\kappa_s|, -(\frac{D_i}{k_i} + \frac{d_s}{k_s})) e^{i\kappa_s \cdot (\rho_a - \rho_B)} \\ &= \frac{1}{(2\pi)^3} (-i) \frac{2\pi}{\frac{D_i}{k_i} + \frac{d_s}{k_s}} G(|\rho_a - \rho_B|, \frac{1}{\frac{D_i}{k_i} + \frac{d_s}{k_s}}) \\ &= \frac{1}{2\pi} \frac{1}{i\lambda_s R_s} G(|\rho_a - \rho_B|, \frac{K_s}{R_s}), \end{aligned} \quad (13)$$

because $\frac{D_i}{k_i} + \frac{d_s}{k_s} = \frac{1}{2\pi} (D_i \lambda_i + d_s \lambda_s) = \frac{\lambda_s}{2\pi} (D_i \frac{\lambda_i}{\lambda_s} + d_s) = \frac{R_s}{K_s}$. The amplitude for joint photon detection at the bucket detector A and the pixel detector B is then

$$\begin{aligned} U_{AB} &= \langle 0 | E_B^{(+)} E_A^{(+)} | \Psi \rangle = -\frac{\gamma}{\lambda_s L_s} e^{i(K_s z_s + K_i z_i - \Omega_s t_A - \Omega_i t_B)} \int d\mathbf{v}_s e^{i\mathbf{v}_s \tau_{BA}} \text{sinc}(\mathbf{v}_s D_{si} \frac{L}{2}) \\ &\times \left\{ \frac{1}{2\pi i \lambda_s R_s} G(|\rho_A|, \frac{K_s}{L_s}) G(|\rho_B|, \frac{K_s}{R_s}) \int d^2 \rho_a t(\rho_a) G(|\rho_a|, K_s (\frac{1}{L_s} + \frac{1}{R_s})) e^{-iK_s (\frac{\rho_B}{R_s} + \frac{\rho_A}{L_s}) \cdot \rho_a} \right\} \\ &\equiv -\frac{\gamma}{\lambda_s L_s} e^{i(K_s z_s + K_i z_i - \Omega_s t_A - \Omega_i t_B)} \int d\mathbf{v}_s e^{i\mathbf{v}_s \tau_{BA}} \text{sinc}(\mathbf{v}_s D_{si} \frac{L}{2}) V(\rho_A, \rho_B). \end{aligned} \quad (14)$$

We now consider the scattering of the optical photon with the atoms in a lattice by integrating over ρ_a , and the collection of optical photons at the bucket detector A by integrating over ρ_A in the detector plane, because the bucket detector collects photons without distinguishing their actual position. We expect that difference patterns can be formed on the image plane of the pixel detector B, with intensity $I(\rho_B)$ and joint photon counting rate $R_c(\rho_B)$ at ρ_B

$$I(\rho_B) = R_c(\rho_B) T \sim \int d^2 \rho_A |V(\rho_A, \rho_B)|^2. \quad (15)$$

To obtain the analogous Bragg equation for two-color biphoton ghost diffraction, we consider two optical paths A_1 and A_2 of the optical photons that scatter with two atoms in two lattice planes with distance $d \equiv d_{hkl}$ (Fig. S1). For optical path A_1 , we have

$$\begin{aligned} L_s^{(1)} &= \Delta \equiv L_s \\ R_s^{(1)} &= d_s + \frac{\lambda_i}{\lambda_s} D_i \equiv R_s, \end{aligned} \quad (16)$$

and for optical path A_2

$$\begin{aligned} L_s^{(2)} &= \Delta + \delta \equiv L_s + \delta \\ R_s^{(2)} &= (d_s + \delta) + \frac{\lambda_i}{\lambda_s} D_i \equiv R_s + \delta, \end{aligned} \quad (17)$$

where $\delta = d \sin \theta$. Thus the effective biphoton joint detection amplitude consists of contribution from the two optical paths, $V(\rho_A, \rho_B) = V^{(1)}(\rho_A, \rho_B) + V^{(2)}(\rho_A, \rho_B)$, and $t(\rho_a) = t^{(1)}(\rho_a) + t^{(2)}(\rho_a) = \psi_0 [\delta(\rho_a - \mathbf{d}) + \delta(\rho_a)]$, where $\mathbf{d} = (d, 0)$. We write $V^{(1)}(\rho_A, \rho_B)$ and $V^{(2)}(\rho_A, \rho_B)$ explicitly as

$$\begin{aligned} V^{(1)}(\rho_A, \rho_B) &= \frac{\psi_0}{2\pi i \lambda_s R_s} G(|\rho_A|, \frac{K_s}{L_s}) G(|\rho_B|, \frac{K_s}{R_s}) G(|\mathbf{d}|, K_s (\frac{1}{L_s} + \frac{1}{R_s})) e^{-iK_s (\frac{\rho_B}{R_s} + \frac{\rho_A}{L_s}) \cdot \mathbf{d}} \\ V^{(2)}(\rho_A, \rho_B) &= \frac{\psi_0}{2\pi i \lambda_s (R_s + \delta)} G(|\rho_A|, \frac{K_s}{L_s + \delta}) G(|\rho_B|, \frac{K_s}{R_s + \delta}). \end{aligned} \quad (18)$$

Take far-field approximation $\delta \ll R_s$ for Laue diffraction, we have

$$\begin{aligned} V(\rho_A, \rho_B) &\simeq \frac{\psi_0}{2\pi i \lambda_s R_s} G(|\rho_A|, \frac{K_s}{L_s}) G(|\rho_B|, \frac{K_s}{R_s}) \\ &\times \left\{ e^{i\frac{K_s}{2} (\frac{1}{L_s} + \frac{1}{R_s}) |\mathbf{d}|^2} e^{-iK_s (\frac{\rho_B}{R_s} + \frac{\rho_A}{L_s}) \cdot \mathbf{d}} + e^{i\frac{K_s}{2} (\frac{1}{L_s + \delta} - \frac{1}{L_s}) |\rho_A|^2} e^{i\frac{K_s}{2} (\frac{1}{R_s + \delta} - \frac{1}{R_s}) |\rho_B|^2} \right\}, \end{aligned} \quad (19)$$

and

$$\begin{aligned}
 |V(\rho_A, \rho_B)|^2 &= \left(\frac{\psi_0}{2\pi\lambda_s R_s} \right)^2 \left\{ 2 + e^{i \left[\frac{K_s}{2} \left(\frac{1}{L_s} + \frac{1}{R_s} \right) |\mathbf{d}|^2 - K_s \left(\frac{\rho_B}{R_s} + \frac{\rho_A}{L_s} \right) \cdot \mathbf{d} + \frac{K_s}{2} \frac{\delta}{L_s^2} |\rho_A|^2 + \frac{K_s}{2} \frac{\delta}{R_s^2} |\rho_B|^2 \right]} + \text{c.c.} \right\} \\
 &= \left(\frac{\psi_0}{2\pi\lambda_s R_s} \right)^2 \{ 2 + I_1 + \text{c.c.} \}.
 \end{aligned} \tag{20}$$

Integrating I_1 in Eq. 20 over ρ_A gives

$$\int d^2 \rho_A \{ I_1 \} = \frac{2\pi i L_s^2}{K_s \delta} e^{i \left[\frac{K_s}{2} \left(\frac{1}{L_s} + \frac{1}{R_s} \right) |\mathbf{d}|^2 - \frac{K_s}{R_s} \rho_B \cdot \mathbf{d} \right]} e^{i \left[\frac{K_s}{2} \frac{\delta}{R_s^2} |\rho_B|^2 - \frac{K_s}{2\delta} |\mathbf{d}|^2 \right]}. \tag{21}$$

Analogous with the procedure in Section II, we obtain the Bragg equation for two-color biphoton ghost diffraction from Eq. 21, by letting the δ dependent phase to be $n\pi$, with an integer n ,

$$\begin{aligned}
 &\frac{K_s}{2} \frac{\delta}{R_s^2} |\rho_B|^2 - \frac{K_s}{2\delta} |\mathbf{d}|^2 \\
 &= \frac{\pi}{\lambda_s} \left[\frac{d \sin \theta}{\left(\frac{d_s}{D_i} + \frac{\lambda_i}{\lambda_s} \right)^2} \frac{|\rho_B|^2}{D_i^2} - \frac{1}{d \sin \theta} \right] = n\pi.
 \end{aligned} \tag{22}$$

We complete the integration of ρ_A over the plane of bucket detector A, with $\rho_B = (x, 0)$ and $\mathbf{d} = (d, 0)$,

$$\begin{aligned}
 \int d^2 \rho_A |V(\rho_A, \rho_B)|^2 &= \left(\frac{\psi_0}{2\pi\lambda_s R_s} \right)^2 \left\{ 2\sigma_A + \frac{2\pi i L_s^2}{K_s \delta} e^{i \left[\frac{K_s}{2} \left(\frac{1}{L_s} + \frac{1}{R_s} \right) |\mathbf{d}|^2 - \frac{K_s}{R_s} \rho_B \cdot \mathbf{d} \right]} + \text{c.c.} \right\} \\
 &= \left(\frac{\psi_0}{2\pi\lambda_s R_s} \right)^2 \left\{ 2\sigma_A + \frac{\pi L_s^2}{K_s \delta} \sin \left[\frac{K_s}{2} \left(\frac{1}{L_s} + \frac{1}{R_s} \right) |\mathbf{d}|^2 - \frac{K_s}{R_s} \rho_B \cdot \mathbf{d} \right] \right\} \\
 &= \left(\frac{\psi_0}{2\pi\lambda_s R_s} \right)^2 \left\{ 2\sigma_A + \frac{\lambda_s L_s^2}{2\delta} \sin \left[\frac{\pi}{\lambda_s} \left(\frac{1}{L_s} + \frac{1}{R_s} \right) d^2 - \frac{2\pi}{\lambda_s R_s} x d \right] \right\},
 \end{aligned} \tag{23}$$

where in Eq. 23

$$\frac{\pi}{\lambda_s} \left(\frac{1}{L_s} + \frac{1}{R_s} \right) d^2 - \frac{2\pi}{\lambda_s R_s} x d = -\frac{2\pi}{\lambda_s R_s} d \left(x - \frac{R_s + L_s}{2L_s} d \right). \tag{24}$$

With Eqs. 1, 7, 14 and 23, we arrive at the final equation for the counting rate of joint photon detection,

$$\begin{aligned}
 R_c(\rho_B) &= \frac{1}{T} \int dt_A dt_B S(t_B, t_A) \frac{\sigma_B \gamma^2}{\lambda_s^2 L_s^2} \left| \int d\mathbf{v}_s e^{i\mathbf{v}_s \cdot \mathbf{r}_{BA}} \text{sinc}(\mathbf{v}_s D_{si} \frac{L}{2}) \right|^2 \int d^2 \rho_A |V(\rho_A, \rho_B)|^2 \\
 &= \frac{1}{T} \int dt_A dt_B S(t_B, t_A) \frac{\gamma^2 \psi_0^2 \sigma_A \sigma_B}{2\pi^2 \lambda_s^4 R_s^4 L_s^4} \\
 &\quad \times \left| \int d\mathbf{v}_s e^{i\mathbf{v}_s \cdot \mathbf{r}_{BA}} \text{sinc}(\mathbf{v}_s D_{si} \frac{L}{2}) \right|^2 \left\{ 1 - \frac{\lambda_s L_s^2}{4d \sin \theta \sigma_A} \sin \left[\frac{2\pi}{\lambda_s R_s} d \left(x - \frac{R_s + L_s}{2L_s} d \right) \right] \right\}.
 \end{aligned} \tag{25}$$

Here a physical counting rate should require either $\frac{\lambda_s L_s^2}{4\delta \sigma_A} \leq 1$, or $\sin \left[\frac{2\pi}{\lambda_s R_s} d \left(x - \frac{R_s + L_s}{2L_s} d \right) \right] \leq 0$.

II. KINEMATIC DESCRIPTION OF LAUE DIFFRACTION

In Section I, the Bragg condition for the two-color biphoton ghost diffraction is obtained from a kinematic scenario. Here we show the conventional Bragg equation can be obtained from similar procedure for the Laue diffraction with monochromatic X-ray beam.

According to Fourier optics, a light wave that passes the plane $z = 0$, and arrives at the plane $z = \Delta$ can be described by the Huygens principle as

$$\begin{aligned}
 \psi(x, y, \Delta) &= \int dk_x dk_y e^{i(k_x x + k_y y)} e^{ik_z \Delta} \mathcal{F}[\psi(x, y, 0)] \\
 &= \int dk_x dk_y e^{i(k_x x + k_y y)} e^{i\Delta \sqrt{k^2 - k_x^2 - k_y^2}} \tilde{\psi}(k_x, k_y, 0) \\
 &\simeq \int dk_x dk_y e^{i(k_x x + k_y y)} e^{i\Delta \left(k - \frac{k_x^2 + k_y^2}{2k}\right)} \tilde{\psi}(k_x, k_y, 0) \\
 &= \mathcal{F}^{-1} \left\{ e^{i\Delta \left(k - \frac{k_x^2 + k_y^2}{2k}\right)} \tilde{\psi}(k_x, k_y, 0) \right\} \\
 &= \psi(x, y, 0) \otimes P(x, y, \Delta),
 \end{aligned} \tag{26}$$

where $P(x, y, \Delta)$ is

$$\begin{aligned}
 P(x, y, \Delta) &= \mathcal{F}^{-1} \left\{ e^{i\Delta k} e^{i\Delta \left(\frac{k_x^2 + k_y^2}{2k}\right)} \right\} \\
 &= -\frac{ik e^{ik\Delta}}{2\pi\Delta} e^{i\frac{k(x^2 + y^2)}{2\Delta}}.
 \end{aligned} \tag{27}$$

The physical scenario of Eq. 26 reflects a typical statement of Huygens principle, that (a) the Fourier transformation on the $z = 0$ plane makes a map to the momentum space $\psi(x, y, 0) \rightarrow \tilde{\psi}(k_x, k_y, 0)$, (b) each Fourier mode $\tilde{\psi}(k_x, k_y, 0)$ corresponds to a sub-source that travels as a plane wave $e^{i(k_x x + k_y y)} e^{ik_z \Delta}$ to the $z = \Delta$ plane, (c) an inverse Fourier transformation on the $z = \Delta$ plane gives the image $\psi(x, y, \Delta)$. For Laue diffraction, we follow a standard treatment by considering two optical paths 1 and 2 for photons that scatter off atoms in two lattice planes (Fig. 2(a)). Assume the photon scatters of the two atoms O and O' with amplitude $t^{(1)} = \psi_0 \delta(x - d, y, 0)$ and $t^{(2)} = \psi_0 \delta(x, y, 0)$, and denote $\delta = d \sin \theta$, we have

$$\begin{aligned}
 \psi_1(x, y, \Delta) &= \psi_0 \otimes P(x - 0, y - d, \Delta) = -\frac{ik\psi_0 e^{ik\Delta}}{2\pi\Delta} e^{i\frac{k}{2\Delta}[(x-d)^2 + y^2]} \\
 \psi_2(x, y, \Delta) &= \int dk_x dk_y e^{ik_z \Delta} \left\{ \int dx dy e^{i(k_x x + k_y y)} \psi_0 \delta(x, y, 0) \right\} e^{ik(\Delta + \delta)} e^{-i(\Delta + \delta) \left(\frac{k_x^2 + k_y^2}{2k}\right)} \\
 &= -\frac{ik\psi_0 e^{ik(\Delta + 2\delta)}}{2\pi(\Delta + 2\delta)} e^{i\frac{k}{2(\Delta + 2\delta)}(x^2 + y^2)}.
 \end{aligned} \tag{28}$$

Thus the intensity of diffraction pattern $I(x)$ at the detector plane is given by

$$\begin{aligned}
 I(x) &= |\psi(x, y, \Delta)|^2 = |\psi_1(x, y, \Delta) + \psi_2(x, y, \Delta)|^2 \\
 &= \left(\frac{k\psi_0}{2\pi}\right)^2 \left\{ \frac{1}{\Delta^2} + \frac{1}{(\Delta + 2\delta)^2} + \frac{1}{\Delta(\Delta + \delta)} \left[e^{i\frac{\pi}{\lambda} \left[\frac{(x-d)^2}{\Delta} - \frac{x^2}{\Delta + 2\delta} \right]} e^{-i\frac{2\pi}{\lambda} 2\delta} + \text{c.c.} \right] \right\} \\
 &= \left(\frac{k\psi_0}{2\pi}\right)^2 I_1.
 \end{aligned} \tag{29}$$

For far-field diffraction $\Delta \gg 2\delta$, we have

$$\begin{aligned}
 I_1 &\simeq \frac{1}{\Delta^2} \left\{ 2 + 2 \cos \left[\frac{\pi}{\lambda \Delta} [(x-d)^2 - x^2] - \frac{2\pi}{\lambda} 2\delta \right] \right\} \\
 &= \frac{2}{\Delta^2} \left\{ 1 + \cos \left[\frac{\pi}{\lambda \Delta} d(d - 2x) - \frac{2\pi}{\lambda} 2\delta \right] \right\} \\
 &= \left(\frac{2}{\Delta}\right)^2 \cos^2 \left[\frac{\pi}{\lambda \Delta} d \left(x - \frac{d}{2}\right) - \frac{\pi}{\lambda} 2\delta \right],
 \end{aligned} \tag{30}$$

using the relation $1 + \cos \alpha = 2 \cos^2 \frac{\alpha}{2}$.

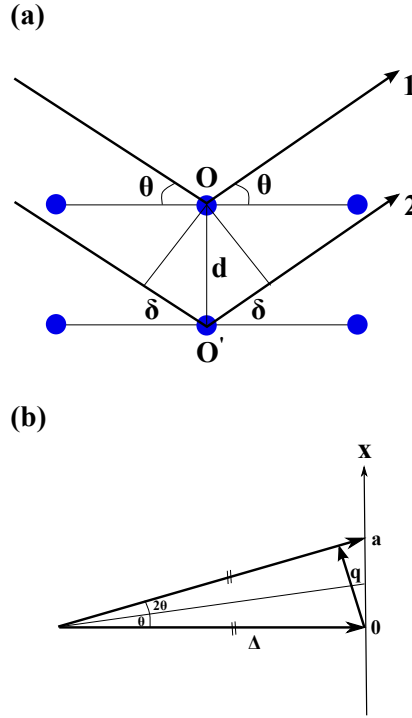


FIG. 2. (a) Optical path diagram for Laue diffraction. (b) Momentum relation of Laue diffraction.

The Bragg condition is obtained by letting the δ dependent phase in Eq. 30 to vanish,

$$2\delta = 2d \sin \theta = n\lambda. \quad (31)$$

We obtain the diffraction pattern on the detector with distance Δ from the sample,

$$I(x) = \left(\frac{k\psi_0}{\pi\Delta} \right)^2 \cos^2 \left[\frac{\pi}{\lambda\Delta} d \left(x - \frac{d}{2} \right) \right], \quad (32)$$

with a period $a = \frac{2\lambda\Delta}{d}$. Meanwhile, we show that the kinematic description is consistent with the description of Laue diffraction in momentum space. The form factor $f(\mathbf{q})$ is a Fourier transformation of charge distribution. For simplicity, we model the atoms as point charges, thus

$$f(\mathbf{q}) = \int d\mathbf{r} e^{i\mathbf{q} \cdot \mathbf{r}} [\delta(\mathbf{r}) + \delta(\mathbf{r} - \mathbf{d})] = 1 + e^{iqd}, \quad (33)$$

and the intensity of diffraction pattern is

$$I \sim |f(\mathbf{q})|^2 = 2(1 + \cos qd) = 4 \cos^2 \frac{qd}{2}. \quad (34)$$

From Fig. 2(b), we can find that $\sin \theta \simeq \frac{x}{2\Delta}$ and

$$q \equiv |\mathbf{q}| = 2|\mathbf{k}| \sin \theta \simeq 2 \frac{2\pi}{\lambda} \frac{x}{2\Delta} = \frac{2\pi x}{\lambda\Delta} \quad (35)$$

Taken Eqs. 34 and 35, we obtain the intensity of diffraction pattern

$$I(x) \sim |f(\mathbf{q})|^2 = 4 \cos^2 \left(\frac{\pi d}{\lambda\Delta} x \right), \quad (36)$$

with a period $a = \frac{2\lambda\Delta}{d}$, which is consistent with Eq. 32 from the kinematic description of Laue diffraction.

III. BROADENING OF BRAGG PEAKS

Because the Bragg peaks of the two-color biphoton ghost diffraction appear at small angles, it is crucial to determine their width in order to justify the resolution of this imaging technique. For a nanocrystal with finite size L , the widths of Bragg peaks are primarily determined by Scherrer equation. Scherrer equation describes diffraction from a realistic crystal with N lattice planes by generalizing the two-slit diffraction (Fig. 1) to the N -slit case, and relates the width of Bragg peak $B = 2\Delta\theta$ with the crystal size L . We show here that the Scherrer equation for two-color biphoton ghost diffraction could allow us to distinguish small angle peaks. For simplicity, instead of calculating the *sinc*-type lineshape of an N -slit ghost diffraction, we adopt here a formal treatment. From the relation $\lambda_s = \frac{d}{\sin\theta}$ and $(N-1)d = L$ we have

$$(N-1)\lambda_s = \frac{(N-1)d}{\sin\theta} = \frac{L}{\sin\theta}. \quad (37)$$

Taken finite difference on both sides of Eq. 37, we obtain

$$0 = \frac{\Delta L}{\sin\theta} - \frac{L \cos\theta \Delta\theta}{\sin^2\theta}. \quad (38)$$

Since $\Delta L = d$, we find

$$B = 2\Delta\theta = \frac{2\lambda_s \sin^2\theta}{L \cos\theta} \quad (39)$$

as the Scherrer equation for the two-color biphoton ghost diffraction.

-
- [1] A. Strekalov, A. V. Sergienko, D. N. Klyshko, and Y. H. Shih, Phys. Rev. Lett. **74**, 3600 (1995).
 - [2] M. H. Rubin and Y. H. Shih, Phys. Rev. A **78**, 033836 (2008).
 - [3] S. Shwartz et al., Phys. Rev. Lett. **109**, 013602 (2012).
 - [4] J. Goodman, *Introduction to Fourier Optics*, Roberts and Company, 2005.
 - [5] M. H. Rubin, Phys. Rev. A **54**, 5349 (1996).